

PEANUT: Perturbations by Eigenvector Alignment for Attacking Graph Neural Networks Under Topology-Driven Message Passing

Bhavya Kohli*

College of Design and Engineering
National University of Singapore
Singapore
bhavyakohli@u.nus.edu

Biplap Sikdar

College of Design and Engineering
National University of Singapore
Singapore
bsikdar@nus.edu.sg

Abstract

Graph Neural Networks (GNNs) have achieved remarkable performance on tasks involving relational data. However, small perturbations to the graph structure can significantly alter GNN outputs, raising concerns about their robustness in real-world deployments. In this work, we explore the core vulnerability of GNNs which explicitly consume graph topology in the form of the adjacency matrix or Laplacian as a means for message passing, and propose PEANUT, a simple, gradient-free, restricted black-box attack that injects *virtual nodes* to capitalize on this vulnerability. PEANUT is an injection based attack, which is widely considered to be more practical and realistic scenario than graph modification attacks, where the attacker is able to modify the original graph structure directly. Our method works at the inference phase, making it an *evasion* attack, and is applicable almost immediately, since it does not involve lengthy iterative optimizations or parameter learning, which add computational and time overhead, or training surrogate models, which are susceptible to failure due to differences in model priors and generalization capabilities. PEANUT also does not require *any* features on the injected node and consequently demonstrates that GNN performance can be significantly deteriorated even with injected nodes with zeros for features, highlighting the significance of effectively designed connectivity in such attacks. Extensive experiments on real-world datasets across three graph tasks demonstrate the effectiveness of our attack despite its simplicity.

CCS Concepts

• Security and privacy → Software and application security; • Theory of computation → Machine learning theory; • Mathematics of computing → Graph algorithms.

Keywords

Graph Neural Networks; Graph Injection Attacks; Black-box Adversarial Attacks; Adversarial Robustness; Graph-level Learning

1 Introduction

Graph Neural Networks (GNNs) have emerged as a central modeling paradigm for learning over relational and structured data across a wide range of applications including molecular property prediction [8, 26], physical simulation [19], traffic forecasting [11, 16], recommendation systems [30], and knowledge graph reasoning [20]. They are increasingly deployed in high-impact settings where adversarial robustness is a practical concern. Their success largely stems

from message passing, where node representations are iteratively updated by aggregating information from local neighborhoods. However, this same mechanism also exposes GNNs to structural vulnerabilities: small, carefully crafted changes in the graph can propagate through the network and lead to significant performance degradation.

Early studies on adversarial attacks against GNNs primarily focus on graph-modification attacks, where the adversary perturbs existing edges or node features [5, 34, 35]. While effective in controlled settings, these attacks often rely on unrealistic assumptions about the attacker’s capability such as having direct access to an existing graph’s topology and being able to modify its attributes. In many real-world systems (e.g., social networks, citation graphs, recommendation systems), modifying existing users, items, or relationships is generally infeasible. In contrast, graph injection attacks provide a more practical threat model where the adversary introduces new nodes into the graph and connects them to existing nodes without altering the original graph structure [13, 22, 24, 32]. Such attacks reflect more realistic scenarios, such as creating fake accounts or synthetic entities to influence downstream performance.

Evasion and poisoning attacks. Depending on the target *phase* (i.e., training or inference), adversarial attacks on GNNs may be categorized into two settings, i.e., poisoning and evasion. In poisoning attacks, the adversary injects malicious nodes into the training graph so that the model is trained on corrupted data and exhibits degraded performance at inference [22, 24, 33]. In evasion attacks, the GNN is assumed to be already trained, and the attacker injects new nodes at test time to manipulate predictions without retraining the model [5, 13, 32]. This paper focuses on the evasion setting, which is particularly relevant for deployed GNN systems where retraining is costly or infrequent, and where adversaries can only interact with the system by introducing new entities at inference.

Vulnerability of adjacency-input architectures. Many widely used GNN architectures explicitly utilize the adjacency (or Laplacian) matrix [7, 15, 25] as message-passing operators. This design choice introduces a major architectural vulnerability: perturbations to the adjacency matrix directly alter the propagation pathways through which information flows, affecting the graph’s receptive fields, aggregation neighborhoods, and spectral properties. This ultimately results in amplified, nonlocal changes in downstream representation. Unlike feature perturbations, which are often normalized or regularized, such adjacency perturbations modify the structure of the computation graph itself.

Despite recent progress on graph injection attacks, most existing methods remain limited in both practicality and scope. A large

*Corresponding Author: Bhavya Kohli
This work is a preprint

fraction of prior work relies on per-graph iterative optimization or reinforcement learning to construct the injected nodes’ features and edges, which is computationally expensive and must be repeated for every target graph or attack instance [17, 22–24]. Moreover, current injection attacks are predominantly evaluated on node-level tasks such as node classification, with limited evidence of effectiveness beyond this narrow setting [13, 22, 23]. Several recent approaches approximate the victim GNN by training surrogate models, which may be insufficient to having different priors and generalization capabilities, while also introducing additional time and resource overhead for their training. This makes the attack pipeline even more cumbersome in practice, and limits its applicability in large-scale or real-time settings.

Contributions. To address the aforementioned drawbacks of previous works, we propose a black-box attack, namely *Perturbation by Eigenvector Alignment for Graph Neural Networks Under Topology-driven message passing* (PEANUT), which works on the evasion setting. Our proposed method can be applied *immediately* to a trained GNN without any per-graph optimization or surrogate model training, only requires the attacker to view the final node-level representations. Furthermore, it generalizes beyond node classification and can be directly applied to GNNs trained for arbitrary graph-level objectives, including the largely underexplored graph regression setting. We summarize our contributions as follows:

- We identify a restricted black-box attack surface induced by GNN architectures that explicitly utilize graph topology matrices for message passing.
- We propose a simple, gradient and surrogate-free, restricted black-box attack that injects virtual nodes to maximize differences between clean and perturbed graph representations.
- We provide the first known systematic evaluation of such attacks on graph-level regression tasks, demonstrating that even small perturbations can meaningfully degrade performance on graph regression benchmarks.

1.1 Threat Model

We consider a *restricted black-box* threat model which works at the inference phase (evasion attack). The attacker has no access to model parameters, gradients, or training data, but can observe only the final node-level representations during inference (e.g. output logits or log-probabilities for a node classifier, node representations prior to graph-pooling operations for graph-level tasks). This setting reflects modular deployment pipelines in which node-level embeddings are utilized by downstream components, while the underlying components themselves remain black boxes. The attacker is allowed to perturb the input graph structure via virtual node injection, subject to a perturbation budget. The goal of the attacker is to induce large deviations in the generated embeddings by constructing perturbed graphs that maximize a discrepancy measure between clean and attacked graph representations.

2 Related works

Structural Attacks on GNNs. Adversarial attacks on graph neural networks (GNNs) frequently target the graph structure by modifying the adjacency matrix through edge additions or deletions.

Early white-box methods assume full access to model parameters and gradients, e.g. Nettack [33] performs targeted perturbations of edges and features to induce misclassifications under structural constraints. Meta-learning-based poisoning attacks optimize the adjacency in a bi-level formulation to maximally degrade downstream performance [35]. Gradient-based topology attacks, such as Fast Gradient Attack (FGA) [2], relax discrete edges into continuous variables and greedily select perturbations via gradients. These approaches demonstrate that small structural changes can significantly impact GNN predictions, but rely on strong white-box assumptions, and work on the graph modification that are unrealistic in many deployment settings. On the other hand, black-box, or *restricted* black-box approaches such as GF-Attack [1], work under more feasible attack assumptions where attackers do not observe model parameters, gradients, or training data, but may assume access to restricted internal representations or confidence scores. Alternative black-box settings with no model queries have also been explored by optimizing surrogate spectral objectives that aim to maximally alter the implicit graph filters induced by GNNs [27]. A few more classical white-box and recent black-box methods are summarized in [3, 12, 21].

Graph Injection Attacks. A growing body of work studies graph injection attacks, where adversaries introduce malicious nodes to degrade GNN performance without modifying existing graph structure. The Node Injection Poisoning Attack (NIPA) [22] injects nodes during training using deep reinforcement learning to sequentially optimize edges and labels under a white-box setting. Due to its high compute requirements, it is considered not scalable for large-scale datasets [32]. Under the black-box setting, Topological Defective Graph Injection Attack (TDGIA) [32] offers a scalable inference-time injection attack that relies on iterative optimization of injected node features and connectivity, however it relies on training surrogate models for its attack mechanism. To maintain the unnoticeability of injection attacks, Chen et al. [4] propose AGIA, a differentiable realization of the graph homophily constraint, showing that constraining injected nodes to match local homophily improves unnoticeability while maintaining their respective attack success. An extremely limited scenario of a single-node injection attack is considered in Tao et al. [23], wherein the objective is to find the most damaging injected node by a carefully crafted optimization scheme. This is further extended as the Generalizable Node Injection Attack model (G-NIA) which can work in black-box settings to amortize the per-graph optimization cost, although requiring a generator model to be trained. The Gradient-free Graph Advantage Actor Critic model (G2A2C) [13] uses reinforcement learning to discover injection policies through repeated interaction with the target model, incurring substantial query and training overhead in the process. QUGIA [17], a Query-based and Unnoticeable Graph Injection Attack, tries to avoid the need to train surrogate models, however it still requires iterative sampling and distribution updates per target graph. Zhou et al. [31] extend graph injection attacks to graph-level classification under a hard-label black-box setting, building upon existing edge perturbing attacks, using query-based optimization to inject nodes that flip graph predictions.

Graph-level tasks and regression. Most prior work on structural attacks focus on node classification, with some exploring the effects

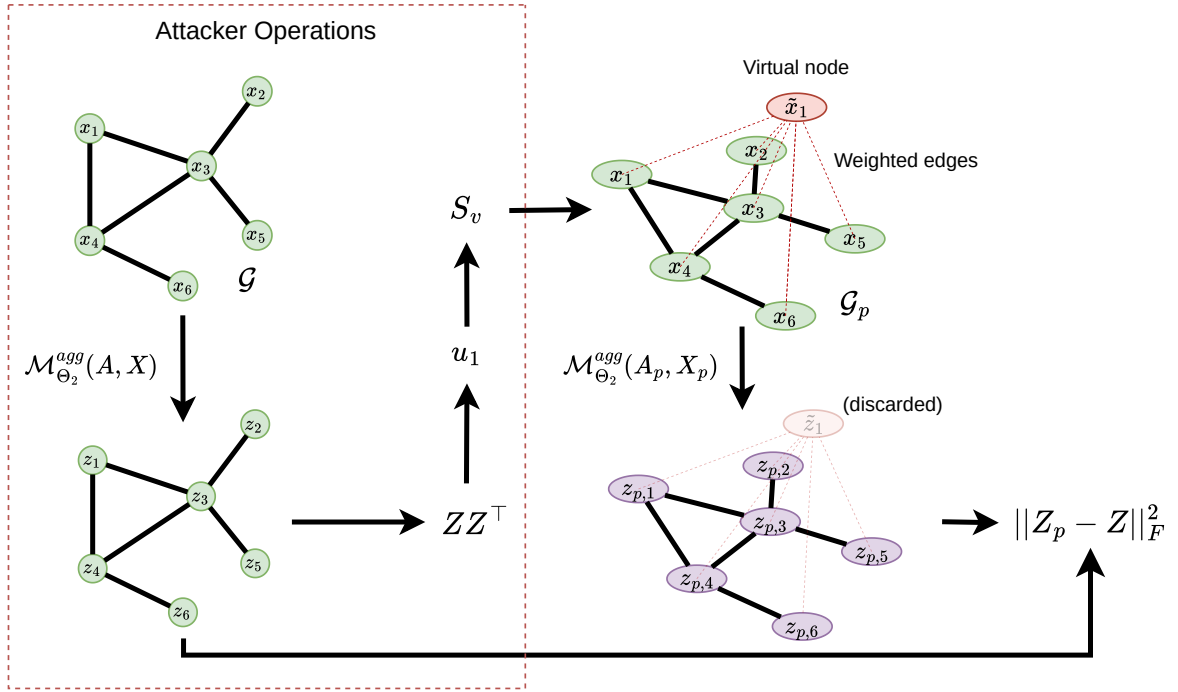


Figure 1: PEA when used on a graph-level task. The attacker queries the model once to obtain the (clean) node-level embeddings, using them to create the perturbation S_v using the eigenvector u_1 of ZZ^T which induces a high $\mathcal{L}(S_v)$.

on graph-level classification. Graph-level regression tasks, such as molecular property prediction or physical system modeling, remain comparatively underexplored in adversarial literature. In contrast to prior black-box approaches that rely on learning-based policies or query-driven optimization, our method leverages final node-level representations to construct gradient-free structural perturbations. We demonstrate that maximizing the norm discrepancy between clean and perturbed graphs constitutes an effective attack objective for graph-level regression, revealing a previously unexplored vulnerability of architectures that explicitly utilize graph topology matrices, such as the adjacency matrix or graph Laplacian, as input. Furthermore, we demonstrate that this sort of norm discrepancy also translates to drops in performance in classification-based tasks.

3 Preliminaries

Let $\mathcal{G}(\mathcal{V}, A, X)$ be an undirected attributed graph with vertex set \mathcal{V} of size N , and adjacency matrix $A \in \mathbb{R}^{N \times N}$ with associated edge set \mathcal{E} . We denote the node attributes of \mathcal{G} as $X \in \mathbb{R}^{N \times D}$, and following the notation in Wu et al. [25], we denote the normalized adjacency matrix as $S = D^{-1/2} A D^{-1/2}$, where D is the diagonal degree matrix of A , and $D_{ii} = \sum_j A_{ij}$. We consider a graph neural network (GNN) with parameters Θ , denoted $\mathcal{M}_{\Theta}(A, X)$, which uses the graph adjacency matrix and node attributes as inputs to produce task-specific outputs.

For node-level tasks, such as node classification with C classes, the network \mathcal{M}_{Θ} outputs log-probabilities (or unnormalized logits)

$Z \in \mathbb{R}^{N \times C}$. For graph-level tasks, we represent the model as a composition

$$\mathcal{M}_{\Theta}(A, X) = \mathcal{M}_{\Theta_1}^{out}(\text{POOL}(\mathcal{M}_{\Theta_2}^{agg}(A, X))), \quad (1)$$

where $\mathcal{M}_{\Theta_2}^{agg}$ first computes node-level embeddings $Z \in \mathbb{R}^{N \times d}$ which are then pooled to produce a single graph-level representation. This pooled embedding is finally reduced by the readout network $\mathcal{M}_{\Theta_1}^{out}$ to either a vector of C values (graph-level classification with C classes), or a single value (graph-level regression). This follows the design flow commonly used in molecular and physical system applications [8, 26].

Virtual-node perturbation. For a graph \mathcal{G} , we define a *virtual-node perturbation* as the adjacency matrix with n_v injected virtual nodes with the real-virtual, virtual-real, and virtual-virtual node connections defined by matrices $A_{r,v}$, $A_{v,r}$, and $A_{v,v}$ respectively. The adjacency matrix of the perturbed graph with $N_p = N + n_v$ nodes is defined as $A_p \in \mathbb{R}^{N_p \times N_p}$. To minimize the number of new edges added, we consider $A_{v,v} = \mathbf{0}^{n_v \times n_v}$, and to maintain symmetry, we consider $A_{r,v} = A_{v,r}^T = A_v \in \mathbb{R}^{N \times n_v}$. Thus, a perturbation is uniquely determined by A_v . If we work with the normalized adjacency matrix S , the perturbed matrix follows the same structure, with S_v instead of A_v . The perturbed matrix is thus defined as:

$$A_p = \begin{pmatrix} A & A_v \\ A_v^T & \mathbf{0} \end{pmatrix}. \quad (2)$$

The feature matrix of the perturbed graph is denoted by $\mathbf{X}_p = (\mathbf{X} \ \tilde{\mathbf{X}})^\top \in \mathbb{R}^{N_p \times D}$. To simplify the closed-form expression in Theorem 1, we assign a vector of zeros to all virtual nodes. We refer to the perturbed graph as \mathcal{G}_p .

Simplified Graph Convolution Network (SGC). The simplified linear version of a Graph Convolution Network (GCN) [15], has been shown to perform similarly, if not better, than GCNs at tasks such as node classification and text classification [25]. Given a 2-Layer SGC, we denote \mathbf{Z} as the node embeddings for an unperturbed graph, i.e., $\mathbf{Z} = \mathbf{S}^2 \mathbf{X} \Theta$. Additionally, we define the node embeddings for the real nodes of a perturbed graph as \mathbf{Z}_p , which is $\mathbf{S}_p^2 \mathbf{X}_p \Theta[: N, :]$, i.e., the first N rows of $\mathbf{S}_p^2 \mathbf{X}_p \Theta$.

Attack Efficacy and Constraints. We define the *attack efficacy* (denoted by $\mathcal{L}(\mathbf{S}_v)$) of perturbation \mathbf{S}_v as the norm of the difference of node embeddings of the real nodes for the original and perturbed graphs, i.e., $\mathcal{L}(\mathbf{S}_v) = \|\mathbf{Z}_p - \mathbf{Z}\|_F^2$. To constrain the perturbation which maximizes \mathcal{L} , we impose a norm constraint $\|\mathbf{S}_v \mathbf{S}_v^\top\|_F \leq \Delta$. If the perturbation \mathbf{S}_v were binary, this would correspond to a bound on the exact number of new edges being added. Our main optimization objective, therefore, is as follows:

$$\begin{aligned} \max_{\mathbf{S}_v \in \mathbb{R}^{N \times n_v}} \quad & \mathcal{L}(\mathbf{S}_v) = \|\mathbf{Z}_p - \mathbf{Z}\|_F^2 \\ \text{s.t.} \quad & \|\mathbf{S}_v \mathbf{S}_v^\top\|_F \leq \Delta \end{aligned} \quad (3)$$

For a Simple Graph Convolution network, $\mathcal{L}(\mathbf{S}_v)$ reduces to the following, assuming $\tilde{\mathbf{X}} = \mathbf{0}$ (See Appendix A.1):

$$\mathcal{L}(\mathbf{S}_v) = \|\mathbf{Z}_p - \mathbf{Z}\|_F^2 = \|\mathbf{S}_v \mathbf{S}_v^\top \mathbf{X} \Theta\|_F^2. \quad (4)$$

3.1 Attack Goal

For the class of GNNs defined above, admitting the adjacency matrix \mathbf{A} (or \mathbf{S} , or graph Laplacian \mathbf{L} , etc.) as the input introduces a structural vulnerability. Our proposed attack injects *virtual nodes* with carefully chosen edge weights, aiming to modify the node-level embeddings \mathbf{Z} and thereby degrading performance on the downstream task. The attack is *gradient-free* and requires no access to model parameters Θ . For node-level tasks, this makes the attack strictly black-box; for graph-level tasks, it relies on observing the intermediate output of $\mathcal{M}_{\Theta_2}^{agg}$, making it a *restricted black-box* method overall. As shown in Section 5.2, this approach is effective across a variety of commonly used architectures, demonstrating that even limited adjacency perturbations can induce substantial changes in graph-level outputs.

4 Methodology

In this section, we define the base version of our method, which, for brevity, we will refer to as **PEA**, for *Perturbation by Eigenvector Alignment*. First, we define a white-box variant for the SGC architecture in Theorem 1 which requires knowledge of the model parameters Θ . We refer to this variant as PEA-W. Then, in Section 4.1, we propose the black-box formulation, which also significantly deteriorates GNN performance. We follow this with a discussion on the practical considerations of generating perturbations in this manner, and comment on the differences in how we should interpret the results for three different graph-based tasks. The flow of

PEA is summarized in Figure 1, and in Algorithms 1-2 in Appendix B.

Before proving the result in Theorem 1, we first need a key result:

LEMMA 1. *For a given real-valued $\mathbf{Z} \in \mathbb{R}^{N \times d}$, and budget Δ , we define the following optimization objective:*

$$\begin{aligned} \max_{\mathbf{B} \in \mathbb{R}^{N \times n}} \quad & \|\mathbf{B} \mathbf{B}^\top \mathbf{Z}\|_F^2 \\ \text{s.t.} \quad & \|\mathbf{B} \mathbf{B}^\top\|_F \leq \Delta \end{aligned} \quad (5)$$

The solution \mathbf{B}^ for the above is $\mathbf{B}^* = \Delta \cdot \mathbf{u}_1 \mathbf{v}^\top$, where \mathbf{u} is the dominant eigenvector (corresponding to the eigenvalue of largest magnitude) of $\mathbf{Z} \mathbf{Z}^\top$, and \mathbf{v} is any unit-norm vector in \mathbb{R}^n .*

PROOF. The proof uses the trace-equivalent representation of the frobenius norm, followed by the eigen-decomposition of $\mathbf{Z} \mathbf{Z}^\top$. See Appendix A for more details. \square

THEOREM 1. *Given a trained 2-Layer Simple Graph Convolution network \mathcal{M}_Θ , and graph $\mathcal{G}(\mathcal{V}, \mathbf{A}, \mathbf{X})$, the perturbation \mathbf{S}_v which maximizes $\mathcal{L}(\mathbf{S}_v)$ while satisfying $\|\mathbf{S}_v \mathbf{S}_v^\top\|_F \leq \Delta$, is given by*

$$\mathbf{S}_v^* = \Delta \cdot \mathbf{u}_1 \mathbf{v}, \quad (6)$$

where \mathbf{u}_1 is the dominant eigenvector of $\mathbf{H} \mathbf{H}^\top$ ($\mathbf{H} = \mathbf{X} \Theta$), and \mathbf{v} is any vector with unit norm.

PROOF. Using the formulation of $\mathcal{L}(\mathbf{S}_v)$ defined for the SGC in Equation 4, we can apply Lemma 1 to obtain \mathbf{S}_v^* . \square

Working with Limited Information. With this simple result, assuming there are no limitations, we can obtain a budget-constrained perturbation \mathbf{S}_v which induces the *maximum* change in the output $\mathbf{Z} = \mathcal{M}_\Theta(\mathbf{A}, \mathbf{X})$. We can, however, make this work in a black-box manner by using \mathbf{Z} instead of \mathbf{H} . Considering the Cauchy-Schwarz inequality and the formulation in Equation 4,

$$\|\mathbf{S}_v \mathbf{S}_v^\top \mathbf{Z}\|_F^2 = \|\mathbf{S}_v \mathbf{S}_v^\top (\mathbf{S}^2 \mathbf{X} \Theta)\|_F^2 \quad (7)$$

$$\leq \|\mathbf{S}^2\|_F^2 \|\mathbf{S}_v \mathbf{S}_v^\top\|_F^2 \|\mathbf{X} \Theta\|_F^2 \quad (8)$$

$$= \|\mathbf{S}^2\|_F^2 \cdot (\Delta^2 \|\mathbf{H}\|_F^2) \quad (9)$$

$$= \|\mathbf{S}^2\|_F^2 \cdot \|\mathbf{S}_v \mathbf{S}_v^\top \mathbf{X} \Theta\|_F^2 \quad (10)$$

Thus, if we assume the attacker only has access to the outputs \mathbf{Z} , maximizing the LHS using Lemma 1 would also push up the RHS, albeit at a lesser effect (see Figure 5).

Choice of \mathbf{v} . For the SGC, the choice of \mathbf{v} has no effect on the outputs since it gets reduced to 1 when computing $\mathbf{S}_v \mathbf{S}_v^\top$. This will not happen in more complex GNN architectures, which may have possible activations or biases inside it, making it a point of further optimization. To keep things simple, however, we only adopt two main methods to obtain \mathbf{v} : (1) Sampling $\mathbf{v} \in \mathbb{R}^{n_v}$ from the standard uniform distribution; and (2) Setting $\mathbf{v} = \mathbf{1}_{n_v}$, i.e., a vector of ones. Both are followed by normalization to unit norm.

Statistic \ Dataset	FreeSolv	ESOL	Lipophilicity	ZINC	AQSOL	MUTAG	PROTEINS	ENZYMES	IMDB-BINARY	BBBP	BACE
Number of Graphs	641	1126	4200	12000	9833	188	1113	600	1000	2039	1513
Number of Classes	-	-	-	-	-	2	2	6	2	2	2
Avg. Number of Nodes	8.73	13.29	27.04	23.16	17.58	17.93	39.06	32.63	19.77	24.06	34.09
Avg. Number of Edges	25.51	40.63	86.04	72.99	53.38	57.52	184.69	156.91	212.84	75.97	107.81
Avg. Degree	2.83	2.98	3.18	3.14	2.98	3.19	4.73	4.86	9.89	3.13	3.17
Avg. Δ for $r = 0.05$	1.28	2.03	4.30	3.65	2.67	2.88	9.23	7.85	10.64	3.80	5.39

Table 1: Dataset summary for the GR and GC tasks.

Norm Differences and its Effectiveness in Classification Tasks. PEA provides a way to augment the graph topology matrix being considered in order to maximize the norm of the difference of node-level representations of a graph. The way PEA performs this does not have any control on *where* all the norm difference goes; for the node classification task, if the effect of perturbation on \mathbf{Z} happen to somehow maintain the relative ranking order, the attack will have no effect on the actual predicted classes at test time. We will see in Section 5.2.1, however, that PEA does display its effectiveness despite this theoretical pitfall. We observe the same for the graph classification task, maximizing norm difference before the read-out model $\mathcal{M}_{\Theta_1}^{out}$ causes enough perturbation to cause significant misclassifications (Section 5.2.3). Compared to the classification datasets, the graph regression task is much more sensitive to such an induced norm change.

Applicability to other GNNs. Consider a 2-layer GIN model with the internal MLP being a Linear-ReLU-Linear (LRL) model with no bias. The forward-direction update would be as follows:

$$\mathbf{H}^{(1)} = \text{MLP}^{(1)} \left(\left((1 + \varepsilon^{(1)}) \cdot \mathbf{I} + \mathbf{A} \right) \mathbf{X} \right), \quad (11)$$

$$\mathbf{Z} = \text{MLP}^{(2)} \left(\left((1 + \varepsilon^{(2)}) \cdot \mathbf{I} + \mathbf{A} \right) \mathbf{H}^{(1)} \right). \quad (12)$$

It has been observed [28] that when the parameters $\varepsilon^{(1)}$, $\varepsilon^{(2)}$ are set to zero, the resulting GIN (denoted GIN-0) consistently outperforms GIN with nonzero, and even trainable ε , in terms of test accuracy. Writing this in the form of weights \mathbf{W}_{1-4} for the two MLP’s, and denoting $\hat{\mathbf{A}} = \mathbf{I} + \mathbf{A}$

$$\mathbf{Z} = \sigma \left(\hat{\mathbf{A}} \mathbf{H}^{(1)} \mathbf{W}_3 \right) \mathbf{W}_4, \quad (13)$$

$$\mathbf{Z} = \sigma \left(\hat{\mathbf{A}} \left(\sigma \left(\hat{\mathbf{A}} \mathbf{X} \mathbf{W}_1 \right) \mathbf{W}_2 \right) \mathbf{W}_3 \right) \mathbf{W}_4. \quad (14)$$

Under a naïve assumption of removing nonlinearities, this shows the exact same form as SGC. We do not actually use this version of GIN since it is essentially the same model as SGC and does not perform as well on graph-level tasks, however, we want to note that the *pathway* for message passing remains somewhat similar. While our theoretical results are established for a specific architecture type, we hypothesize that exploiting the message-passing mechanism in the same way remains effective even if the specific model incorporates internally complex message passing mechanisms compared to the SGC, and validate this empirically in Section 5.2.

4.1 Practical Considerations

4.1.1 Perturbations With Negative Edge Weights. In the above, we do not constrain positivity on the generated perturbation \mathbf{S}_v , and using eigenvector \mathbf{u}_1 means that there is no control over whether

the perturbation will be positive or not. In principle, if a GNN simply admits an adjacency matrix as input with no restrictions or checks on whether edge weights are non-negative, this would not be an issue. However, considering that these perturbations may be simply “defended” by using one ReLU call on the adjacency matrix before the propagation steps, we assume as such, and try to minimize the number of perturbation connections which are zeroed out. This makes the generated perturbations positive with values $\in [0, 1]$. To this end, we first switch the *direction* of \mathbf{u}_1 to have the maximum number of positive terms as follows: \mathbf{u}_1 is assigned a sign based on the number of positive and negative elements in it, using $\mathbf{u}_1 = \mathbf{u}_1 \cdot \text{sign}(\sum \text{sign}(\mathbf{u}_1))$. With this operation, the eigenvalue ordering remains unaffected as the magnitude is unchanged. The method of obtaining \mathbf{v} defined above ensures that the number of surviving elements does not experience further change after the $\Delta \cdot \mathbf{u}_1 \mathbf{v}^T$ product. We refer to this as the base method (PEA), and refer to the unconstrained version where models simply admit an adjacency matrix without imposing positivity as PEA-U.

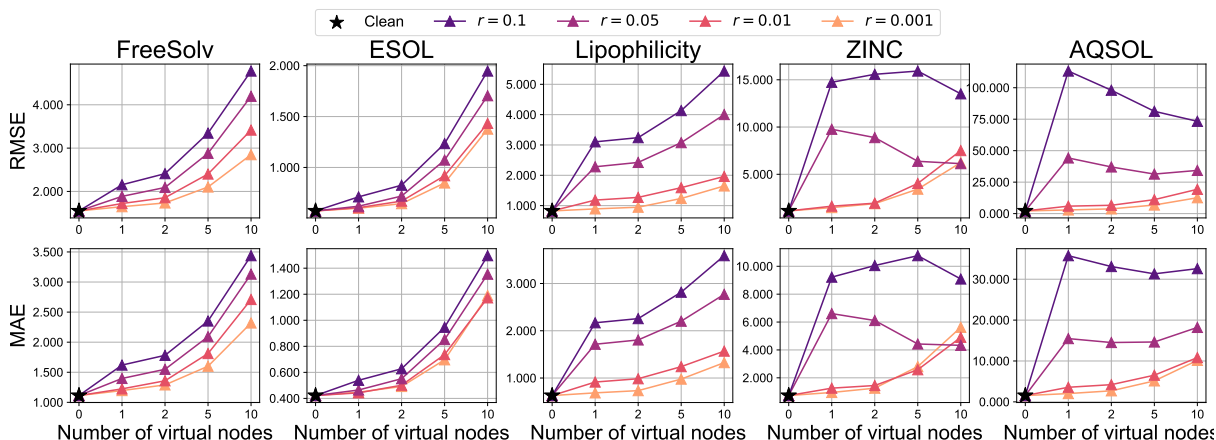
4.1.2 Architectures Which Admit Only Binary Adjacency. In case the GNN does not explicitly utilize edge weights (GIN, SAGE, etc.) and essentially processes the adjacency matrix as if it were binary, we discretize the generated perturbation \mathbf{A}_v by picking the top- k entries for each virtual node where $k = \max(\text{round}(\Delta/n_v), 1)$. Since we have lesser means to distribute the available budget in this discrete case, we assign at least one edge for each virtual node, making the minimum possible perturbation equal to $2n_v$ (n_v each for \mathbf{S}_v and \mathbf{S}_v^T). This is usually only relevant on graph datasets with smaller graphs, where a low $r = 0.01$ may correspond to a value less than 1. The effective budget Δ' in this case is essentially $n_v \Delta$. We refer to this version of PEA as PEA-D

5 Experiments

In this section, we empirically evaluate PEANUT on three graph tasks—Node Classification (NC), Graph Classification (GC), and Graph Regression (GR).

5.1 Experimental Setup

5.1.1 Datasets. We evaluate the efficacy of PEA on NC using the three benchmark citation networks—Cora, Citeseer, and Pubmed [29], and compare its performance with baselines. Then, we evaluate PEA on five benchmark regression datasets—ESOL, FreeSolv, and Lipophilicity [26], ZINC [9], and AQSOL [6], and on GC using four benchmark graph classification datasets from TUDataset [18]—MUTAG, PROTEINS, ENZYMES, and IMDB-BINARY, and two datasets from MoleculeNet [26]—BBBP and BACE, for a total of six datasets spanning molecular property prediction, social networks,


Figure 2: GIN Regression performance vs number of virtual nodes on the five regression datasets.

Dataset	r	n_v	Clean Graph		AGIA		TDGIA		ATDGIA		PEA (Ours)	
			Accuracy	F1 Score	Accuracy \downarrow	F1 \downarrow	Accuracy \downarrow	F1 \downarrow	Accuracy \downarrow	F1 \downarrow	Accuracy \downarrow	F1 \downarrow
Cora	0.001	2			0.04 \pm 0.11	0.03 \pm 0.08	0.07 \pm 0.15	0.05 \pm 0.10	0.07 \pm 0.15	0.07 \pm 0.15	0.07 \pm 0.17	0.04 \pm 0.17
	0.01	27			2.52 \pm 0.62	2.21 \pm 0.62	2.41 \pm 0.48	2.04 \pm 0.56	<u>3.78\pm0.92</u>	<u>5.11\pm1.69</u>	0.72 \pm 0.42	0.57 \pm 0.42
	0.05	135	78.48 \pm 2.53	72.77 \pm 4.92	8.96 \pm 1.18	10.24 \pm 1.58	9.81 \pm 1.55	11.05 \pm 1.89	12.78 \pm 2.25	13.55 \pm 2.24	<u>36.12\pm1.94</u>	<u>45.34\pm3.18</u>
	0.1	270			12.44 \pm 1.30	13.38 \pm 1.69	13.00 \pm 1.45	13.72 \pm 1.88	14.52 \pm 2.00	15.05 \pm 2.35	<u>51.65\pm0.77</u>	<u>73.08\pm0.77</u>
Citeseer	0.001	3			0.15 \pm 0.15	0.11 \pm 0.11	0.15 \pm 0.15	0.11 \pm 0.11	<u>0.18\pm0.15</u>	<u>0.17\pm0.13</u>	0.00 \pm 0.07	-0.00 \pm 0.06
	0.01	33			2.26 \pm 0.28	2.03 \pm 0.24	<u>2.32\pm0.52</u>	<u>2.08\pm0.48</u>	1.99 \pm 0.63	1.92 \pm 0.58	0.26 \pm 0.52	0.45 \pm 0.70
	0.05	166	77.68 \pm 0.89	67.38 \pm 1.33	8.61 \pm 0.45	7.68 \pm 0.44	8.49 \pm 0.87	7.58 \pm 0.73	12.92 \pm 0.68	11.23 \pm 0.59	<u>15.16\pm6.65</u>	<u>17.97\pm6.46</u>
	0.1	332			11.05 \pm 0.82	9.66 \pm 0.74	10.81 \pm 0.61	9.55 \pm 0.57	14.61 \pm 1.44	12.62 \pm 1.22	<u>37.64\pm7.82</u>	<u>45.38\pm8.29</u>
Pubmed	0.001	19			0.04 \pm 0.02	0.03 \pm 0.03	0.02 \pm 0.02	0.03 \pm 0.03	0.03 \pm 0.09	0.02 \pm 0.11	<u>0.21\pm0.14</u>	<u>0.33\pm0.17</u>
	0.01	197			0.76 \pm 0.26	0.76 \pm 0.26	0.72 \pm 0.26	0.72 \pm 0.31	1.10 \pm 0.10	1.16 \pm 0.15	<u>4.33\pm0.76</u>	<u>7.24\pm1.48</u>
	0.05	985	85.80 \pm 0.24	84.71 \pm 0.24	3.99 \pm 0.37	4.14 \pm 0.41	3.78 \pm 0.51	3.88 \pm 0.51	10.22 \pm 1.08	10.65 \pm 1.11	<u>34.24\pm4.64</u>	<u>50.24\pm5.42</u>
	0.1	1971			11.98 \pm 1.14	12.39 \pm 1.30	11.54 \pm 0.97	11.88 \pm 1.19	11.98 \pm 1.13	12.29 \pm 1.31	<u>41.78\pm1.56</u>	<u>61.09\pm2.35</u>

Table 2: Results of PEA and the baselines on Node classification using the GCN architecture as the defending model. The accuracy and (macro) F1 score on the clean datasets are reported first, followed by their respective decrease for each method.

biophysics and physiology. We summarize some key statistics of these datasets in Tables 3 and 1.

Statistic \ Dataset	Cora	Citeseer	Pubmed
Number of Classes	7	6	3
Number of Nodes	2708	3327	19717
Number of Edges	10556	9104	88648
Avg. Degree	4.90	3.74	5.50
n_v for $r = 0.01$	27	33	197
Δ for $r = 0.01$	132	124	1083

Table 3: Dataset summary for the NC task.

5.1.2 Metrics. For the regression datasets, we report the test RMSE and MAE; and for the classification datasets, we compute the accuracy and macro-averaged F1 score (denoted by F1) on the test set, both as percents. Unless otherwise mentioned, all reported numbers have been averaged over 10 runs.

5.1.3 Attack Budgets. For NC, we follow the budget allowances as in Sun et al. [22], keeping the number of virtual nodes $n_v = r \cdot |V|$ and

$\Delta = r \cdot |V| \cdot \text{deg}(\mathcal{G})$, where $\text{deg}(\mathcal{G})$ is the average degree of the graph. For GC and GR, we consider the budget Δ available to the attacker as a fraction r of the number of edges of each individual graph, i.e., $\Delta = r \cdot |\mathcal{E}^{(i)}|$ for graph $\mathcal{G}^{(i)}$, and we vary $n_v \in [0, 1, 2, 5, 10]$.

5.1.4 Baselines. Since node injection attacks remain underexplored on the GC and GR tasks, we compare the performance of PEA with baselines on the well-studied and benchmarked NC task. We use TDGIA [32], ATDGIA, a variant of TDGIA proposed by [4], and AGIA [4] as three key baselines. TDGIA involves topological defective edge selection followed by feature learning using smooth adversarial optimization. AGIA requires gradient information (via the surrogate) to learn the features and structures of the injected nodes. For a fair comparison, we impose our attack budget constraints defined in Section 5.1.3 for deciding the number of injected nodes and the corresponding perturbation budget.

5.1.5 Architectures. For NC, we use the SGC [25], GCN [15], GIN [28], and SAGE [10] architectures for evaluating the effects of PEA-style perturbations across models with different propagation styles.

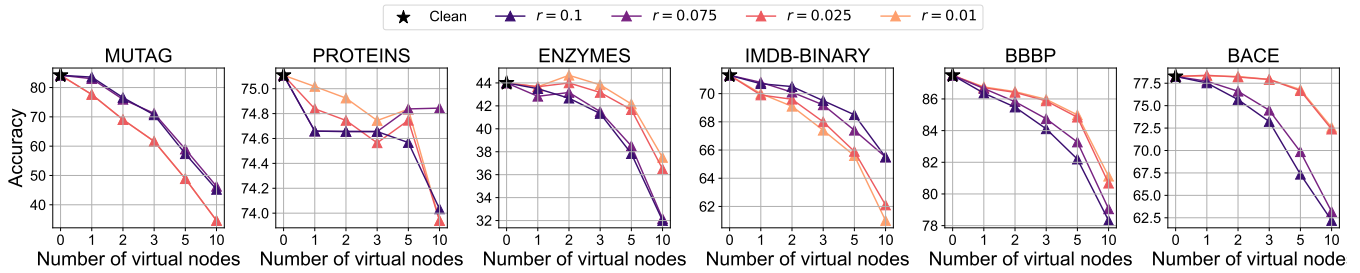


Figure 3: GIN Classification accuracy vs number of virtual nodes on the six classification datasets. All reported numbers have been averaged over the 10-Fold CV.

The GIN, and SAGE architectures usually do not admit the adjacency matrix as-is since they only deal with unattributed aggregation over neighbors. However common implementations often use products of the form AX as a parallelizable and efficient aggregation step, which is an exploitable vulnerability for PEA. The architecture of choice for graph-level tasks will be a 2-layer GIN. However, for a few simple graph-regression datasets, we also train a GCN to confirm our performance trends. For all tasks, each architecture described consists of 2 graph convolution layers of the specified architecture.

5.2 Results

Dataset	Model	r	n_v	Accuracy (F1)	Accuracy \downarrow (F1 \downarrow)
Cora	SGC	0.05	135	83.77(82.42)	35.97(45.52)
		0.1	270	83.77(82.42)	52.03(73.76)
	GCN	0.05	135	83.33(81.71)	38.28(49.63)
		0.1	270	83.33(81.71)	51.70(73.37)
	GIN	0.05	135	79.30(76.63)	44.44(64.49)
		0.1	270	79.30(76.63)	47.97(68.12)
	SAGE	0.05	135	84.01(82.56)	5.71(5.94)
		0.1	270	84.01(82.56)	10.61(11.36)
Citeseer	SGC	0.05	166	75.32(71.53)	7.50(10.09)
		0.1	332	75.32(71.53)	31.40(36.49)
	GCN	0.05	166	74.86(71.12)	13.83(16.98)
		0.1	332	74.86(71.12)	36.45(43.75)
	GIN	0.05	166	68.11(64.27)	50.18(57.43)
		0.1	332	68.11(64.27)	45.29(51.89)
	SAGE	0.05	166	74.86(70.73)	1.65(2.34)
		0.1	332	74.86(70.73)	3.22(4.33)
Pubmed	SGC	0.05	985	83.09(82.40)	35.10(50.94)
		0.1	1971	83.09(82.40)	41.54(60.94)
	GCN	0.05	985	83.63(82.96)	36.15(52.43)
		0.1	1971	83.63(82.96)	42.25(61.84)
	GIN	0.05	985	75.84(67.66)	35.84(46.54)
		0.1	1971	75.84(67.66)	37.09(48.37)
SAGE	0.05	985	85.27(84.99)	1.94(2.22)	
	0.1	1971	85.27(84.99)	3.43(4.08)	

Table 4: Performance of PEA on NC across GNN architectures.

5.2.1 Node Classification. In Table 2., we compare the performance of PEA with the current state-of-the-art baselines. Despite not being designed explicitly for node classification, and with the pitfalls discussed in Section 4 when dealing with classification-based tasks, PEA performs well across the board, and significantly outperforms the baselines on slightly higher budgets ($\sim 5\%$ injected nodes). Note that the GCN architecture here is assumed to be one which normalizes the adjacency matrix inside. If we assume a model which expects the normalized adjacency matrix S_v as input, and we are able to perturb that directly, we observe an astonishing accuracy (F1 score) drop of over 52(74)% on the Cora dataset, with Citeseer experiencing a 43(54)% drop, and Pubmed experiencing a 43(63)% drop, even with r set as low as 0.001. In Table 4, we apply PEA to the four different GNN architectures, over two values of r .

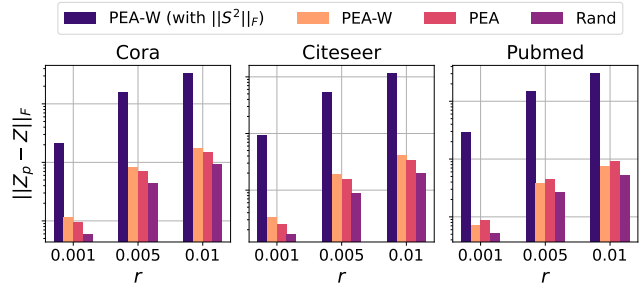


Figure 5: Norm difference ($\mathcal{L}(S_v)$) between PEA-W, PEA, and a randomly chosen S_v , illustrating how the white-box version compares with the black-box approximation and randomly chosen perturbations, using SGC on the NC datasets.

In Figure 5, we compare the perturbation effect $\mathcal{L}(S_v)$ for the NC datasets, supporting the result of Theorem 1 and demonstrating that the black-box approximation in Equations 7-10 does follow the expected trends of when accounting for $\|S^2\|_F$. However, note that the approximation and consequently maximizing the LHS in Equation 7 does indeed lead to a comparable, and in the case of Pubmed, better, $\mathcal{L}(S_v)$ compared to the PEA-W.

5.2.2 Graph Regression. For the regression task, we implement two main model classes: (1) A simple 2-layer GCN, and (2) A 2-layer GIN. As mentioned in Section 5.1.5, although our main architecture is GIN, we train a GCN on the relatively easier datasets to confirm our hypotheses on performance trends.

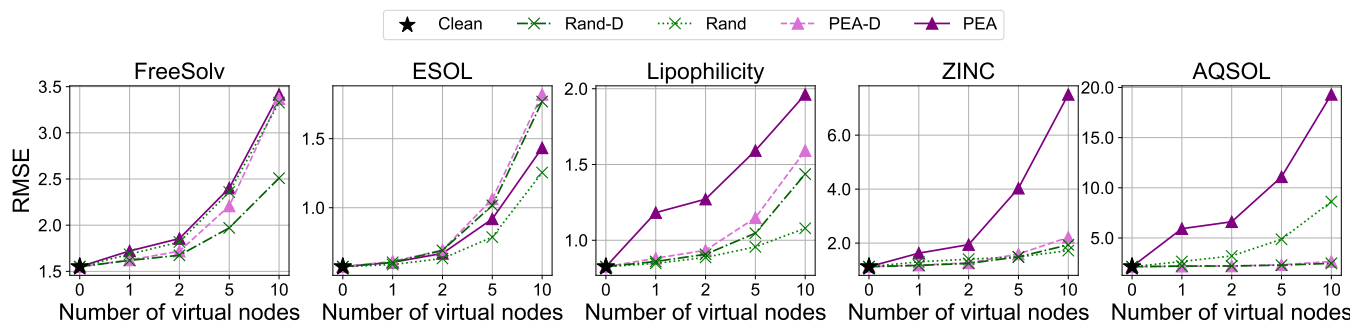


Figure 4: GIN Regression performance for PEA, PEA-D, Rand and Rand-D for the same budget (normalized for the discrete variants), across the five regression datasets.

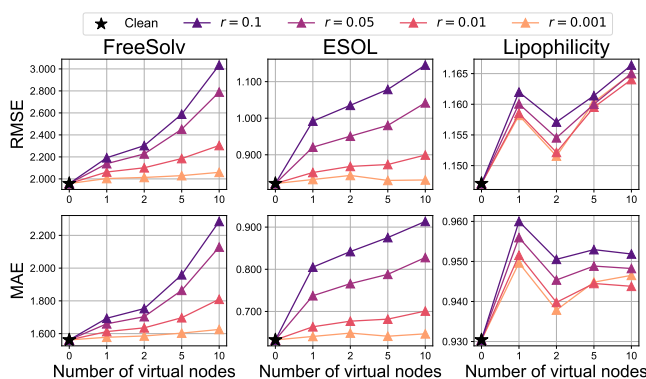


Figure 6: GCN Regression performance vs number of virtual nodes on the MoleculeNet datasets.

In Figure 6, we observe the expected degradation in regression performance when the number of injected nodes and perturbation budgets are increased for the GCN. Despite having much better performance on the base task, In Figure 2, we see the same trends for the GIN, lending some empirical support to our hypothesis that exploiting the message-passing mechanism in the way described works even for architectures with different internal architectures (Section 4.1). In Figure 4, we compare our base method with three alternatives: the discrete variant PEA-D discussed in 4.1, Rand, which corresponds to a randomly generated A_v , and Rand-D, which is discretized in the same fashion as PEA-D.

5.2.3 Graph Classification. For graph classification, we use the GIN due to its significant performance over other architectures across all datasets. In Table 5, we have the accuracy and F1 scores on the clean datasets. In Figure 3, similar to the GR task, we observe a drop in accuracy as we increase the number of injected nodes. In this task, we see that increasing the budget does not always lead to a further drop in performance (notably, in the IMDB-BINARY and MUTAG datasets). This occurs due to how PEA works with norms and not explicitly targeting a certain class, leading to cases where increasing the norm difference of a certain model output may very well place *more* weight on the output logits (or probabilities) corresponding to the correct class, thus not affecting the model’s

prediction. Even in this case, however, we *do* observe performance drops, albeit not following expected trends.

Datasets	Accuracy	F1 Score
MUTAG	84.18±8.12	81.10±10.75
PROTEINS	75.11±2.43	73.67±2.32
ENZYMES	44.00±8.10	42.94±6.65
IMDB-BINARY	71.30±3.80	71.05±3.84
BBBP	87.49±1.49	81.24±3.43
BACE	78.26±3.26	77.93±3.39

Table 5: Mean test accuracy on clean datasets using a GIN. Statistics are computed over 10-Fold cross validation splits.

6 Conclusion

In this work, we study graph injection attacks in a practical black-box setting with access to node-level embeddings and explicit budget constraints on injected node connections. Due to its formulation and lack of computational prerequisites, our method is designed to be immediately applicable to any deployed GNN, without requiring surrogate model training, reinforcement learning, or per-graph iterative optimization. Across a range of architectures and tasks, including underexplored graph-level objectives such as graph regression, our approach consistently degrades model performance under tight injection budgets, while maintaining efficiency and ease of deployment.

Empirically, our results follow expected trends: attack effectiveness increases with budget in most cases, and models that rely more heavily on local neighborhood aggregation, especially if they explicitly consume graph topology matrices as-is, are more vulnerable to carefully crafted virtual node injections. Compared to strong baselines our method achieves competitive, and even better performance under the same budget constraints while substantially reducing computational overhead and attack latency, avoiding the nontrivial setup and runtime costs associated with surrogate models or iterative optimizations, which limit their practicality in large-scale or time-sensitive scenarios. Our method closes much of this performance gap without these costs, making it better suited for real-world evasion settings. In future, we would like to explore ways to improve the performance of the discrete variants, and applying this to more complex GNN architectures.

References

- [1] Heng Chang, Yu Rong, Tingyang Xu, Wenbing Huang, Honglei Zhang, Peng Cui, Wenwu Zhu, and Junzhou Huang. 2020. A Restricted Black-box Adversarial Framework Towards Attacking Graph Embedding Models. In *Proceedings of the Thirty-Fourth AAAI Conference on Artificial Intelligence*. 11132–11139.
- [2] Jinyin Chen, Yangyang Wu, Xuanheng Xu, Yixian Chen, Haibin Zheng, and Qi Xuan. 2018. Fast gradient attack on network embedding. *arXiv preprint arXiv:1809.02797* (2018).
- [3] Liang Chen, Jintang Li, Jiaying Peng, Tao Xie, Zengxu Cao, Kun Xu, Xiangnan He, Zibin Zheng, and Bingzhe Wu. 2020. A survey of adversarial learning on graphs. *arXiv preprint arXiv:2003.05730* (2020).
- [4] Yongqiang Chen, Han Yang, Yonggang Zhang, Kaili Ma, Tongliang Liu, Bo Han, and James Cheng. 2022. Understanding and improving graph injection attack by promoting unnoticeability. *arXiv preprint arXiv:2202.08057* (2022).
- [5] Hanjun Dai, Hui Li, Tian Tian, Xin Huang, Lin Wang, Jun Zhu, and Le Song. 2018. Adversarial attack on graph structured data. In *International conference on machine learning*. PMLR, 1115–1124.
- [6] Vijay Prakash Dwivedi, Chaitanya K Joshi, Anh Tuan Luu, Thomas Laurent, Yoshua Bengio, and Xavier Bresson. 2023. Benchmarking graph neural networks. *Journal of Machine Learning Research* 24, 43 (2023), 1–48.
- [7] Guoji Fu, Peilin Zhao, and Yatao Bian. 2022. p -Laplacian Based Graph Neural Networks. In *International conference on machine learning*. PMLR, 6878–6917.
- [8] Justin Gilmer, Samuel S Schoenholz, Patrick F Riley, Oriol Vinyals, and George E Dahl. 2017. Neural message passing for quantum chemistry. In *International conference on machine learning*. Pmlr, 1263–1272.
- [9] Rafael Gómez-Bombarelli, Jennifer N Wei, David Duvenaud, José Miguel Hernández-Lobato, Benjamín Sánchez-Lengeling, Dennis Sheberla, Jorge Aguilera-Iparraguirre, Timothy D Hirzel, Ryan P Adams, and Alán Aspuru-Guzik. 2018. Automatic chemical design using a data-driven continuous representation of molecules. *ACS central science* 4, 2 (2018), 268–276.
- [10] Will Hamilton, Zhitao Ying, and Jure Leskovec. 2017. Inductive representation learning on large graphs. *Advances in neural information processing systems* 30 (2017).
- [11] Weiwei Jiang and Jiayun Luo. 2022. Graph neural network for traffic forecasting: A survey. *Expert systems with applications* 207 (2022), 117921.
- [12] Wei Jin, Yaxing Li, Han Xu, Yiqi Wang, Shuiwang Ji, Charu Aggarwal, and Jiliang Tang. 2021. Adversarial attacks and defenses on graphs. *ACM SIGKDD Explorations Newsletter* 22, 2 (2021), 19–34.
- [13] Mingxuan Ju, Yujie Fan, Chuxu Zhang, and Yanfang Ye. 2023. Let graph be the go board: gradient-free node injection attack for graph neural networks via reinforcement learning. In *Proceedings of the AAAI conference on artificial intelligence*, Vol. 37. 4383–4390.
- [14] Diederik P Kingma and Jimmy Ba. 2014. Adam: A method for stochastic optimization. *arXiv preprint arXiv:1412.6980* (2014).
- [15] TN Kipf. 2016. Semi-supervised classification with graph convolutional networks. *arXiv preprint arXiv:1609.02907* (2016).
- [16] Yaguang Li, Rose Yu, Cyrus Shahabi, and Yan Liu. 2017. Diffusion convolutional recurrent neural network: Data-driven traffic forecasting. *arXiv preprint arXiv:1707.01926* (2017).
- [17] Chang Liu, Hai Huang, Yujie Xing, and Xingquan Zuo. 2025. Query-Based and Unnoticeable Graph Injection Attack from Neighborhood Perspective. *arXiv preprint arXiv:2502.01936* (2025).
- [18] Christopher Morris, Nils M Kriege, Franka Bause, Kristian Kersting, Petra Mutzel, and Marion Neumann. 2020. TUDataset: A collection of benchmark datasets for learning with graphs. *arXiv preprint arXiv:2007.08663* (2020).
- [19] Alvaro Sanchez-Gonzalez, Jonathan Godwin, Tobias Pfaff, Rex Ying, Jure Leskovec, and Peter Battaglia. 2020. Learning to Simulate Complex Physics with Graph Networks. In *Proceedings of the 37th International Conference on Machine Learning (Proceedings of Machine Learning Research, Vol. 119)*, Hal Daumé III and Aarti Singh (Eds.). PMLR, 8459–8468.
- [20] Michael Schlichtkrull, Thomas N Kipf, Peter Bloem, Rianne Van Den Berg, Ivan Titov, and Max Welling. 2018. Modeling relational data with graph convolutional networks. In *European semantic web conference*. Springer, 593–607.
- [21] Lichao Sun, Yingdong Dou, Carl Yang, Kai Zhang, Ji Wang, Philip S Yu, Lifang He, and Bo Li. 2022. Adversarial attack and defense on graph data: A survey. *IEEE Transactions on Knowledge and Data Engineering* 35, 8 (2022), 7693–7711.
- [22] Yiwei Sun, Suhang Wang, Xianfeng Tang, Tsung-Yu Hsieh, and Vasant Honavar. 2020. Adversarial attacks on graph neural networks via node injections: A hierarchical reinforcement learning approach. In *Proceedings of the Web Conference 2020*. 673–683.
- [23] Shuchang Tao, Qi Cao, Huawei Shen, Junjie Huang, Yunfan Wu, and Xueqi Cheng. 2021. Single node injection attack against graph neural networks. In *Proceedings of the 30th ACM International Conference on Information & Knowledge Management*. 1794–1803.
- [24] Jihong Wang, Minnan Luo, Fnu Suya, Jundong Li, Zijiang Yang, and Qinghua Zheng. 2020. Scalable attack on graph data by injecting vicious nodes. *Data Mining and Knowledge Discovery* 34, 5 (2020), 1363–1389.
- [25] Felix Wu, Amauri Souza, Tianyi Zhang, Christopher Fifty, Tao Yu, and Kilian Weinberger. 2019. Simplifying Graph Convolutional Networks. In *Proceedings of the 36th International Conference on Machine Learning (ICML)*. PMLR, 6861–6871.
- [26] Zhenqin Wu, Bharath Ramsundar, Evan N Feinberg, Joseph Gomes, Caleb Geniesse, Aneesh S Pappu, Karl Leswing, and Vijay Pande. 2018. MoleculeNet: a benchmark for molecular machine learning. *Chemical science* 9, 2 (2018), 513–530.
- [27] Jiarong Xu, Yizhou Sun, Xin Jiang, Yanhao Wang, Yang Yang, Chunping Wang, and Jiangang Lu. 2020. Query-Free Black-Box Adversarial Attacks on Graphs. *CoRR abs/2012.06757* (2020).
- [28] Keyulu Xu, Weihua Hu, Jure Leskovec, and Stefanie Jegelka. 2018. How powerful are graph neural networks? *arXiv preprint arXiv:1810.00826* (2018).
- [29] Zhilin Yang, William Cohen, and Ruslan Salakhudinov. 2016. Revisiting semi-supervised learning with graph embeddings. In *International conference on machine learning*. PMLR, 40–48.
- [30] Rex Ying, Ruining He, Kaifeng Chen, Pong Eksombatchai, William L Hamilton, and Jure Leskovec. 2018. Graph convolutional neural networks for web-scale recommender systems. In *Proceedings of the 24th ACM SIGKDD international conference on knowledge discovery & data mining*. 974–983.
- [31] Yu Zhou, Zihao Dong, Guofeng Zhang, and Jingchen Tang. 2023. Hard Label Black Box Node Injection Attack on Graph Neural Networks. *arXiv preprint arXiv:2311.13244* (2023).
- [32] Xu Zou, Qinkai Zheng, Yuxiao Dong, Xinyu Guan, Evgeny Kharlamov, Jialiing Lu, and Jie Tang. 2021. TDGIA: Effective Injection Attacks on Graph Neural Networks. In *Proceedings of the 27th ACM SIGKDD Conference on Knowledge Discovery & Data Mining*. 3428–3438.
- [33] Daniel Zügner, Amir Akbarnejad, and Stephan Günnemann. 2018. Adversarial Attacks on Neural Networks for Graph Data. In *Proceedings of the 24th ACM SIGKDD International Conference on Knowledge Discovery & Data Mining*. ACM, 2847–2856.
- [34] Daniel Zügner, Oliver Borchert, Amir Akbarnejad, and Stephan Günnemann. 2020. Adversarial attacks on graph neural networks: Perturbations and their patterns. *ACM Transactions on Knowledge Discovery from Data (TKDD)* 14, 5 (2020), 1–31.
- [35] Daniel Zügner and Stephan Günnemann. 2019. Adversarial Attacks on Graph Neural Networks via Meta Learning. In *International Conference on Learning Representations (ICLR)*.

A Proof of Lemma 1

LEMMA 1. For a given real-valued $\mathbf{Z} \in \mathbb{R}^{N \times d}$, and budget Δ , we define the following optimization objective:

$$\begin{aligned} \max_{\mathbf{B} \in \mathbb{R}^{N \times n}} \quad & \|\mathbf{B}\mathbf{B}^\top \mathbf{Z}\|_F^2 \\ \text{s.t.} \quad & \|\mathbf{B}\mathbf{B}^\top\|_F \leq \Delta \end{aligned} \quad (15)$$

The solution \mathbf{B}^* for the above is $\mathbf{B}^* = \Delta \cdot \mathbf{u}_1 \mathbf{v}^\top$, where \mathbf{u} is the dominant eigenvector (corresponding to the eigenvalue of largest magnitude) of $\mathbf{Z}\mathbf{Z}^\top$, and \mathbf{v} is any unit-norm vector in \mathbb{R}^n .

PROOF.

$$\begin{aligned} \|\mathbf{B}\mathbf{B}^\top \mathbf{Z}\|_F^2 &= \text{tr}((\mathbf{B}\mathbf{B}^\top \mathbf{Z})^\top (\mathbf{B}\mathbf{B}^\top \mathbf{Z})) \\ &= \text{tr}(\mathbf{Z}^\top \mathbf{B}\mathbf{B}^\top \mathbf{B}\mathbf{B}^\top \mathbf{Z}) \\ &= \text{tr}((\mathbf{B}\mathbf{B}^\top)^2 \mathbf{Z}\mathbf{Z}^\top) \end{aligned}$$

Since $\mathbf{Z}\mathbf{Z}^\top$ is real and symmetric, it allows an eigendecomposition $\mathbf{U}\mathbf{A}\mathbf{U}^\top$. This gives,

$$\begin{aligned} \|\mathbf{B}\mathbf{B}^\top \mathbf{Z}\|_F^2 &= \text{tr}((\mathbf{B}\mathbf{B}^\top)^2 \mathbf{U}\mathbf{A}\mathbf{U}^\top) \\ &= \text{tr}((\mathbf{U}^\top \mathbf{B}\mathbf{B}^\top \mathbf{U})^2 \mathbf{A}) \end{aligned}$$

Denoting $Y = U^T B B^T U$,

$$\begin{aligned} \|\mathbf{B}\mathbf{B}^T \mathbf{Z}\|_F^2 &= \text{tr}(Y^2 \Lambda) \\ &= \sum_i \Lambda_{ii} (Y^2)_{ii} \\ &= \sum_i \lambda_i (Y^2)_{ii} \\ &= \sum_i \sum_j \lambda_i Y_{ij}^2 \end{aligned}$$

The RHS here is a weighted sum of eigenvalues λ_i with weights given by Y_{ij}^2 . The constraint $\|\mathbf{B}\mathbf{B}^T\|_F^2 \leq \Delta^2$ is equivalent to $\|Y\|_F^2 \leq \Delta^2$ due to orthogonality, which may be written as $\sum_i \sum_j Y_{ij}^2 \leq \Delta^2$.

Thus, to maximize the weighted sum given the constraints on the weights, the optimal solution is one where the weights concentrate on the maximum λ_i ($= \lambda_1$). Therefore,

$$\begin{aligned} Y^* &= \Delta \cdot \mathbf{e}_1 \mathbf{e}_1^T \\ \mathbf{B}^* \mathbf{B}^{*\top} &= \Delta \cdot \mathbf{u}_1 \mathbf{u}_1^T \end{aligned}$$

This gives $\mathbf{B}^* = \Delta \cdot \mathbf{u}_1 \mathbf{v}^T$, where \mathbf{v} may be any vector with unit norm (\mathbf{v} has no effect on $\mathbf{B}^* \mathbf{B}^{*\top}$). \square

A.1 Equivalent Formulation of \mathcal{L} for SGC

We have the node embeddings \mathbf{Z} for a clean graph given by $\mathbf{Z} = \mathbf{S}^2 \mathbf{X} \Theta$. For a perturbation \mathbf{S}_v , we have the node embeddings given by $\mathbf{S}_v^2 \mathbf{X}_p \Theta$, which is:

$$\begin{pmatrix} \mathbf{S} & \mathbf{S}_v \\ \mathbf{S}_v^\top & \mathbf{0} \end{pmatrix} \begin{pmatrix} \mathbf{S} & \mathbf{S}_v \\ \mathbf{S}_v^\top & \mathbf{0} \end{pmatrix} \begin{pmatrix} \mathbf{X} \\ \tilde{\mathbf{X}} \end{pmatrix} \Theta = \begin{pmatrix} \mathbf{S}^2 + \mathbf{S}_v \mathbf{S}_v^\top & \mathbf{S} \mathbf{S}_v \\ \mathbf{S}_v^\top \mathbf{S} & \mathbf{S}_v^\top \mathbf{S}_v \end{pmatrix} \begin{pmatrix} \mathbf{X} \\ \tilde{\mathbf{X}} \end{pmatrix} \Theta \quad (16)$$

Extracting the embeddings of the real nodes, i.e., the first N rows of the above, we have:

$$\mathbf{Z}_p = \mathbf{S}^2 \mathbf{X} \Theta + \mathbf{S}_v \mathbf{S}_v^\top \mathbf{X} \Theta + \mathbf{S} \mathbf{S}_v \tilde{\mathbf{X}} \Theta \quad (17)$$

$$\mathbf{Z}_p = \mathbf{Z} + \mathbf{S}_v \mathbf{S}_v^\top \mathbf{X} \Theta + \mathbf{S} \mathbf{S}_v \tilde{\mathbf{X}} \Theta \quad (18)$$

This gives us,

$$\|\mathbf{Z}_p - \mathbf{Z}\|_F^2 = \|\mathbf{S}_v \mathbf{S}_v^\top \mathbf{X} \Theta + \mathbf{S} \mathbf{S}_v \tilde{\mathbf{X}} \Theta\|_F^2 \quad (19)$$

$$\leq \|\mathbf{S}_v \mathbf{S}_v^\top \mathbf{X} \Theta\|_F^2 + \|\mathbf{S} \mathbf{S}_v \tilde{\mathbf{X}} \Theta\|_F^2 \quad (20)$$

Specifically, for $\tilde{\mathbf{X}} = \mathbf{0}$,

$$\|\mathbf{Z}_p - \mathbf{Z}\|_F^2 = \|\mathbf{S}_v \mathbf{S}_v^\top \mathbf{X} \Theta\|_F^2 \quad (21)$$

B Algorithmically describing PEA

In Algorithms 1 and 2, we denote K as the number of test graphs. The function `DOMEIGVEC` returns the dominant eigenvector (corresponding to the eigenvalue with maximum magnitude) of the input. For the other variants of PEA, \mathbf{A}_v is modified before the Insertion step.

C Hyperparameters

C.1 Node Classification

All models trained for NC (SGC, GCN, GIN, and SAGE) consist of two graph convolution layers of the respective type, with the ReLU activation between them for all models except SGC. The latent dimension for all datasets is fixed to 16, and there is no Linear

Algorithm 1 PEA for NC with a single large graph.

Input: Graph $\mathcal{G}(\mathbf{V}, \mathbf{A}, \mathbf{X})$ with N nodes, Budget ratio r

Output: Perturbed Graph $\mathcal{G}_p(\mathbf{V}_p, \mathbf{A}_p, \mathbf{X}_p)$

- 1: $\mathbf{Z} \leftarrow \mathcal{M}_\Theta(\mathbf{A}, \mathbf{X})$
 - 2: $\mathbf{u}_1 \leftarrow \text{DOMEIGVEC}(\mathbf{Z}\mathbf{Z}^\top)$
 - 3: /* Aligning \mathbf{u}_1 along the direction which maintains maximum positive items */
 - 4: $\mathbf{u}_1 \leftarrow \mathbf{u}_1 \cdot \text{sign}(\sum \text{sign}(\mathbf{u}_1))$
 - 5: $n_v \leftarrow \text{floor}(rN)$, $\Delta \leftarrow \text{floor}(rN \cdot \text{deg}(\mathcal{G}))$
 - 6: $\mathbf{v} \sim \mathcal{U}(0, 1)^{\times n_v}$
 - 7: $\mathbf{A}_v \leftarrow \text{ReLU}(\Delta \cdot \mathbf{u}_1 \mathbf{v}^\top)$
 - 8: $\tilde{\mathbf{X}} \leftarrow \mathbf{0}^{n_v \times D}$
 - 9: $\mathbf{A}_p \leftarrow \begin{pmatrix} \mathbf{A} & \mathbf{A}_v \\ \mathbf{A}_v^\top & \mathbf{0} \end{pmatrix}$, $\mathbf{X}_p \leftarrow \begin{pmatrix} \mathbf{X} \\ \tilde{\mathbf{X}} \end{pmatrix}$ ▷ Insertion
 - 10: $\mathcal{G}_p \leftarrow (\mathcal{V} \cup \{n_v\}, \mathbf{A}_p, \mathbf{X}_p)$
-

Algorithm 2 PEA for Graph-level tasks.

Input: Test Set of Graphs $\mathcal{G}^{(1)}, \mathcal{G}^{(2)}, \dots, \mathcal{G}^{(K)}$, Trained GNN \mathcal{M}_Θ . Budget ratio r , Number of virtual nodes n_v

Output: Perturbed graphs $\mathcal{G}_p^{(1)}, \mathcal{G}_p^{(2)}, \dots, \mathcal{G}_p^{(K)}$

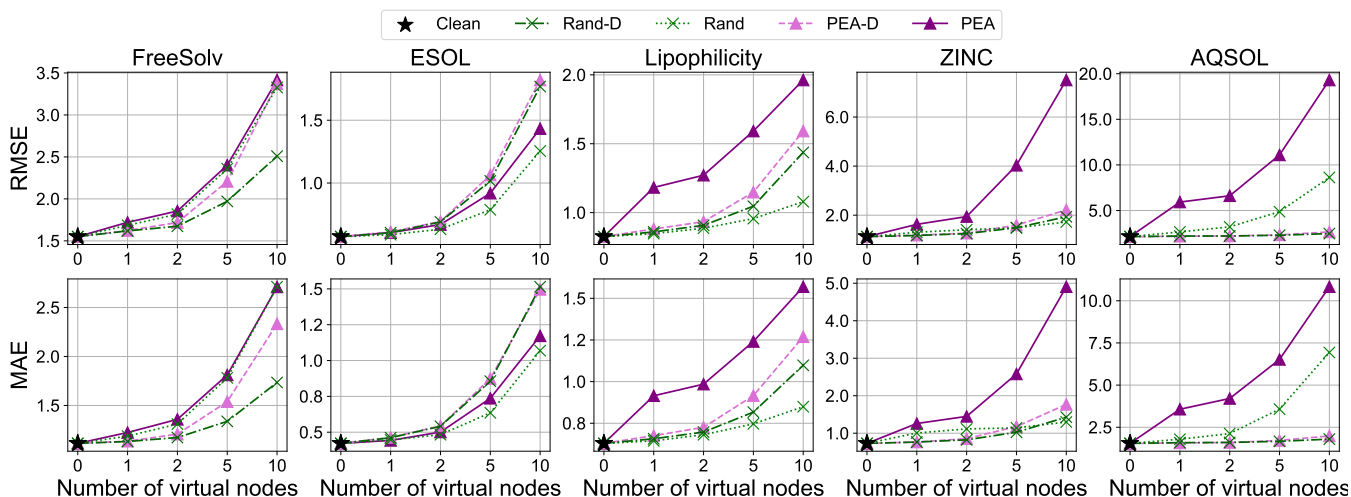
- 1: **for** $i \in [1, \dots, K]$ **do** ▷ Graphs can also be batched
 - 2: $\mathbf{Z} \leftarrow \mathcal{M}_{\Theta_2}^{(agg)}(\mathbf{A}^{(i)}, \mathbf{X}^{(i)})$
 - 3: $\mathbf{u}_1 \leftarrow \text{DOMEIGVEC}(\mathbf{Z}\mathbf{Z}^\top)$
 - 4: $\mathbf{u}_1 \leftarrow \mathbf{u}_1 \cdot \text{sign}(\sum \text{sign}(\mathbf{u}_1))$ ▷ Aligning \mathbf{u}_1 along the direction which maintains maximum positive items
 - 5: $\mathbf{v} \sim \mathcal{U}(0, 1)^{\times n_v}$
 - 6: $\mathbf{v} \leftarrow \frac{\mathbf{v}}{\|\mathbf{v}\|_F}$
 - 7: $\Delta \leftarrow \text{floor}(r \cdot |\mathcal{E}^{(i)}|)$
 - 8: $\mathbf{A}_v \leftarrow \text{ReLU}(\Delta \cdot \mathbf{u}_1 \mathbf{v}^\top)$
 - 9: $\tilde{\mathbf{X}} \leftarrow \mathbf{0}^{n_v \times D}$
 - 10: $\mathbf{A}_p \leftarrow \begin{pmatrix} \mathbf{A} & \mathbf{A}_v \\ \mathbf{A}_v^\top & \mathbf{0} \end{pmatrix}$, $\mathbf{X}_p \leftarrow \begin{pmatrix} \mathbf{X} \\ \tilde{\mathbf{X}} \end{pmatrix}$ ▷ Insertion
 - 11: $\mathcal{G}_p^{(i)} \leftarrow (\mathcal{V} \cup \{n_v\}, \mathbf{A}_p, \mathbf{X}_p)$
 - 12: **end for**
-

readout layer after the second graph convolution. All models are trained using the Adam optimizer [14] with a fixed learning rate of 0.001, and early stopping with patience 100.

C.2 Graph-level tasks: Classification and Regression

All models trained for graph-level tasks (GCN and GIN) consist of two graph convolution layers of the respective type, with the ReLU activation between them. This comprises the $\mathcal{M}_{\Theta_2}^{(agg)}$ portion of the model. The representations are pooled using Add-pooling, and then fed into the readout module, which is a simple LRL with the output either being a single value (GR) or a set of logits (GC) equal to the number of classes. All models are trained using the Adam optimizer [14] with a starting learning rate of 0.001, reduced by a factor of $\gamma = 0.9$ if the tracked validation metric—F1 score for GC, RMSE for GR—does not improve for 20 epochs (plateau lr reduction), with the minimum lr set to $1e-4$. We also use early stopping here with the same patience of 100 epochs.

Dataset	Model	r	n_v	Accuracy	F1 Score	Accuracy \downarrow	F1 \downarrow
Cora	SGC	0.05	135	83.77 \pm 0.39	82.42 \pm 0.40	35.97 \pm 1.71	45.52 \pm 2.94
		0.1	270	83.77 \pm 0.39	82.42 \pm 0.40	52.03 \pm 0.41	73.76 \pm 0.50
	GCN	0.05	135	83.33 \pm 0.59	81.71 \pm 0.67	38.28 \pm 4.20	49.63 \pm 6.05
		0.1	270	83.33 \pm 0.59	81.71 \pm 0.67	51.70 \pm 0.51	73.37 \pm 0.79
	GIN	0.05	135	79.30 \pm 2.03	76.63 \pm 4.73	44.44 \pm 5.32	64.49 \pm 8.03
		0.1	270	79.30 \pm 2.03	76.63 \pm 4.73	47.97 \pm 4.48	68.12 \pm 5.22
SAGE	0.05	135	84.01 \pm 0.71	82.56 \pm 0.85	5.71 \pm 1.13	5.94 \pm 1.35	
	0.1	270	84.01 \pm 0.71	82.56 \pm 0.85	10.61 \pm 1.68	11.36 \pm 2.07	
Citeseer	SGC	0.05	166	75.32 \pm 0.35	71.53 \pm 0.38	7.50 \pm 5.49	10.09 \pm 4.88
		0.1	332	75.32 \pm 0.35	71.53 \pm 0.38	31.40 \pm 11.13	36.49 \pm 11.76
	GCN	0.05	166	74.86 \pm 0.42	71.12 \pm 0.40	13.83 \pm 6.14	16.98 \pm 6.53
		0.1	332	74.86 \pm 0.42	71.12 \pm 0.40	36.45 \pm 7.77	43.75 \pm 7.67
	GIN	0.05	166	68.11 \pm 3.16	64.27 \pm 3.62	50.18 \pm 5.25	57.43 \pm 5.47
		0.1	332	68.11 \pm 3.16	64.27 \pm 3.62	45.29 \pm 10.21	51.89 \pm 10.78
SAGE	0.05	166	74.86 \pm 0.51	70.73 \pm 0.57	1.65 \pm 0.69	2.34 \pm 0.71	
	0.1	332	74.86 \pm 0.51	70.73 \pm 0.57	3.22 \pm 0.86	4.33 \pm 0.98	
Pubmed	SGC	0.05	985	83.09 \pm 0.39	82.40 \pm 0.42	35.10 \pm 2.02	50.94 \pm 2.43
		0.1	1971	83.09 \pm 0.39	82.40 \pm 0.42	41.54 \pm 0.73	60.94 \pm 1.15
	GCN	0.05	985	83.63 \pm 0.47	82.96 \pm 0.44	36.15 \pm 3.06	52.43 \pm 3.96
		0.1	1971	83.63 \pm 0.47	82.96 \pm 0.44	42.25 \pm 0.83	61.84 \pm 1.30
	GIN	0.05	985	75.84 \pm 10.05	67.66 \pm 16.17	35.84 \pm 7.73	46.54 \pm 16.50
		0.1	1971	75.84 \pm 10.05	67.66 \pm 16.17	37.09 \pm 7.12	48.37 \pm 16.00
SAGE	0.05	985	85.27 \pm 0.31	84.99 \pm 0.28	1.94 \pm 0.22	2.22 \pm 0.34	
	0.1	1971	85.27 \pm 0.31	84.99 \pm 0.28	3.43 \pm 0.36	4.08 \pm 0.61	

Table 6: Performance of PEA on NC across GNN architectures, with reported deviations across 10 runs.

Figure 7: GIN Regression performance (RMSE and MAE) for PEA, PEA-D, Rand and Rand-D for the same budget (normalized for the discrete variants), across the five regression datasets.

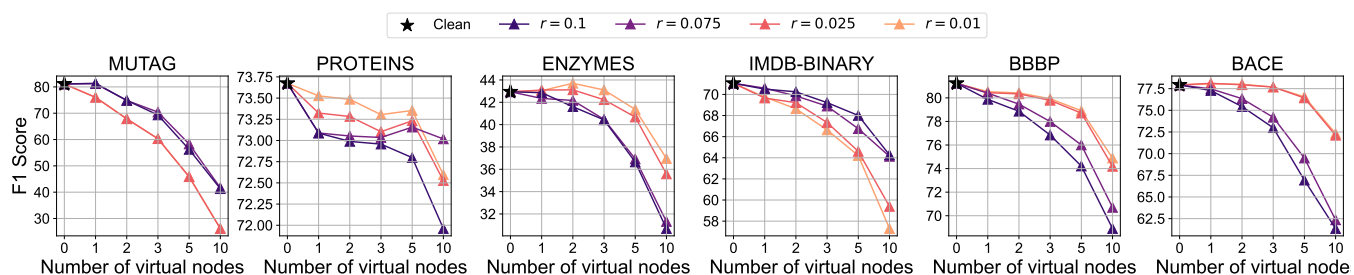


Figure 8: GIN Classification F1 vs number of virtual nodes on the six classification datasets. All reported numbers have been averaged over the 10-Fold CV.

D Additional results

- In Table 6, we include the standard deviations of all metrics over 10 runs.
- In Figure 8, we plot the F1 score vs number of injected virtual nodes, compared to the Accuracy which was shown in Figure 3.
- In Figure 7, we also observe similar trends as Figure 4, on the MAE metric.